Electric field detection using solid state variable capacitance

Maciej A. Noras

University of North Carolina at Charlotte
Dept. of Engineering Technology
phone: (1) 704-687-5053
email: mnoras@uncc.edu

***Abstract*— Operation of traditional fieldmeters typically relies on mechanically actuated capacitance for DC fields measurement. This paper provides theoretical background for operation of an electric field sensor with a solid state variable capacitor. Design is supported by circuit and FEA models, illustrating the operation. Theoretical work is verified against results of sensor's tests performed in DC, AC and pulse electric fields.**

I. Introduction

Low frequency AC and DC electric field measurements can be done in a broad variety of ways, utilizing variety of physical phenomena: induction, force, electroptical effects (Kerr or Pockels), flow of ions (in radiation based devices). The existing instruments can also be divided into two classes: long range and short range sensors. This classification reflects the way the sensor is used, and some instruments can be used in both far and near field detection. The meaning of "far" and "near field" used here is somewhat different from the traditional definition used in electromagnetic field theory, as it is impossible to define a wavelength for a DC and for an impulse electric field that these sensors can measure. In this manuscript the focus is on on methods that use capacitive coupling (induction) to the electric field. These techniques can be classified as 1) dynamic induced current/voltage sensors and 2) Kelvin probe sensors.
Dynamic sensors require changes in the electric field in order to be able to detect the field. Standard techniques for near and far field measurement, employed here, involve an antenna coupled to a voltage or current measuring instrument. These techniques were extensively described in the literature [1, 2, 3]. Passive sensors relying on the variation of electric

field find numerous applications in, for example, detection of moving objects [4, 5], electrostatic discharges (ESD) phenomena [6], electromagnetic field due to seismic activity [[7], etc.
Kelvin probe-based sensors do not rely solely on change of the electric field. Instead, the probe operation depends on change of the capacitive coupling between the field and the sensor. In this way an electric current is induced in the probe, and the magnitude of that current is proportional to the magnitude of the electric field [8]. In fieldmeters and electrostatic voltmeters the capacitance is formed by the instrument's sensor and the object that is being measured. In 1932 Zisman [9] introduced the vibrating Kelvin probe. This technique became a base for contemporary Kelvin probe techniques, including Kelvin force microscopes (KFMs)[10, 11]. The mechanical motion of the sensor needs to be precisely controlled, to assure proper measurement accuracy of the meters. Another way of changing the capacitance was by intermittently inserting a grounded shutter plate in front of the sensor, either in a form of a rotating vane or using a shuttle mechanism. The fieldmeters with a rotating vane or mechanically vibrating sensors [12, 13, 14], are used in broad range of applications, for example in assessment of the electrostatic discharge (ESD) threats [15], atmospheric research [16], etc. Fieldmeters are not very sensitive, and their bandwidth is limited by the velocity of the rotating vane or the vibration frequency of the sensor, with the maximum reaching about 20 Hz [17]. The fieldmeters technical capabilities are not sufficient for application in the projectile sensing. Electrostatic voltmeters (ESVM) are much more sensitive and precise than fieldmeters with the bandwidth of up to 3 kHz [17]. Their construction, however, is relatively expensive and complicated. In both cases limitation comes from the fact that they use mechanical modulation of the capacitance. There are, however, several electronic devices that can have their capacitances controlled electronically: a varactor (a.k.a. varicap), a MOS (metal-oxide-semiconductor) or a MIS (metal-insulator-semiconductor) structure. The idea of using varactors for direct/contacting low current measurements was introduced in 1979 by Herscovici [18] and commercialized by Hewlett Packard in their 4140B pA Meter/DC Voltage Source [19]. The MOS electrometer for current measurements was described by several authors [20]. With some modifications the same method can be utilized in non-contacting electric potential measurements [21]. This paper gives a theoretical background and describes implementation of this sensing technique.

II. Sensing technique theory

The electric field sensing system under consideration can be represented as a diagram shown in Figure 1. The object under test, which is the source of an electric field, is capacitively coupled (C_{op}) to the sensing

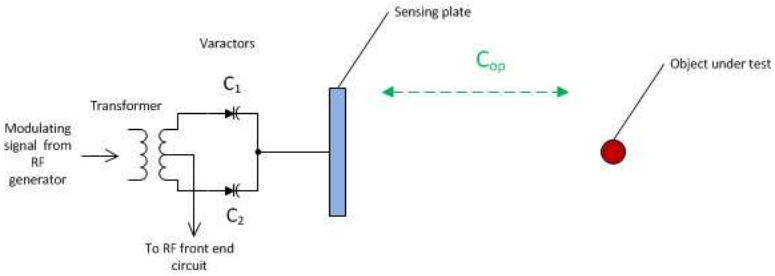

Fig. 1. Sensor's front-end circuit.

plate of the sensor. The plate is a common node for a varactor couple. The varactors are being fed with an RF carrier signal through a center tap transformer. In this way the RF generator and the sensing part of the circuit are galvanically separated. This setup can be portrayed as a circuit presented in Figure 2, where the generator and the transformer are replaced by two voltage sources V(t). Both varactor cathodes are connected to the sensing element at the node A. Together they form a variable, voltage-dependent capacitor. The sensing plate is coupled to ground (C_{pg}), and to the object under test (C_{op}). Assuming that the object has a fixed electric charge Q, the voltage with respect to ground will depend on its capacitive coupling to the ground and to the sensing plate. The sensing plate potential is floating at the average value of the carrier signal - which is zero. Since the plate size is relatively small, it can be assumed that the object's potential depends only on the capacitance of the object to the earth ground, C_{og}. The capacitance C_{pg} can be neglected. The circuit operates in a way similar to the amplitude modulator.

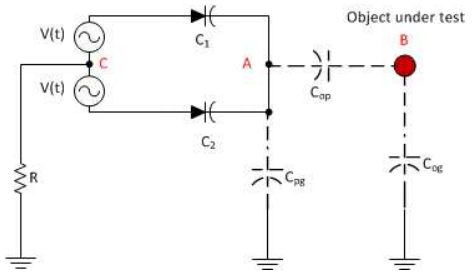

Fig. 2. Equivalent circuit diagram of the varactor sensor front end.

The sinusoidal RF carrier signal applied to varactors is modulated by the electric field signal coming from the object under test. To illustrate the circuit operation, an arbitrarily selected value of 3 kHz AC signal source is being used in place of the object under test, as shown in PSpice simulation, Figure 3. The values for the RF voltage sources were selected

based upon the measurements made on a prototype of the circuit. Capacitor $C_1 = C_{op}$ value had been selected based on results of modeling using the Comsol Multiphysics software for a spherical object, 1 cm in diameter, at 2 m distance from the sensing plate. That particular FEA model was developed for the sensor's application in projectile detection [22], and in this manuscript only some of the modeling results are utilized for the sake of showing the concept of the sensor's operation. The resulting

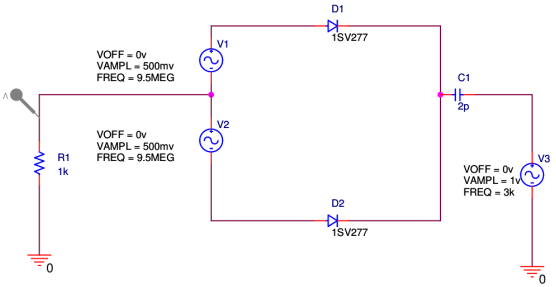

Fig. 3. PSpice front end circuit used in the sensor's circuit simulation.

output current through resistor R is shown in Figure 4. The envelope of the current signal carries the information on the sensed voltage signal (3 kHz sine in this case). This signal then is amplified and demodulated to recover the voltage produced by the object under test. Consider Figure 5representing the theoretical base for the sensor operation. The varactor components are replaced with an equivalent voltage-dependent capacitor in series with the object-to-plate capacitance. Let's represent the capacitors by their respective impedances. An additional assumption is being made here: signal $V_o(t)$ of the tested object is much slower than the carrier signal $V(t)$, and it is treated (for simplicity) as a DC signal during the Laplace transformation. Writing the Kirchhoff's current equation for this circuit yields

$$I(t) = \frac{V(t) - V_o(t)}{Z_{Cv} + R + Z_{Cop}} \tag{1}$$

which is equivalent to

$$I(s) = \frac{\frac{V \cdot \omega}{s^2 + \omega^2} - \frac{V_o}{s}}{Z_{Cv}(s) + R + \frac{1}{s \cdot C_{op}}}, \tag{2}$$

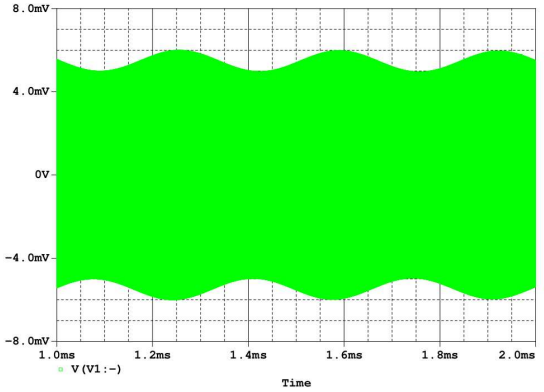

Fig. 4. Simulated output voltage, 3 kHz, 1 V p-p input signal in place of the sensed object's signal.

where V is the magnitude and ω is the circular frequency of the sinusoidal voltage source representing the carrier signal. Recall that the capacitance C_v of the varactor is a nonlinear function of the reverse voltage V_r [23]:

$$C_v = \frac{C_{j0}}{\left(1 + \frac{V_r}{V_j}\right)^M} \tag{3}$$

Parameters C_{jO} (zero-bias junction capacitance), M (grading coefficient) and V_j (junction potential) have to be experimentally determined for a given type of varactor. The prototype design uses 1SV277 [24] varactors, for which the parameters were measured as: M=1.7, V_j=3.5 V, C_{j0}=6.9

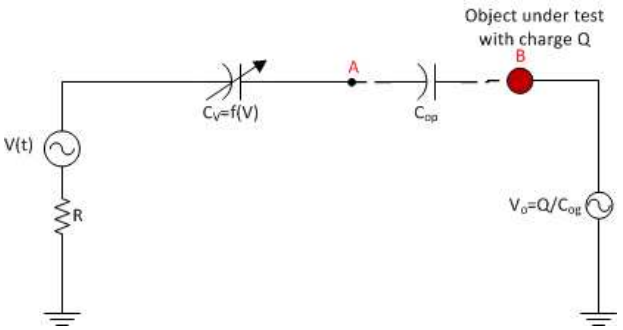

Fig. 5. PSpice equivalent circuit used in demonstrating variable capacitance concept.

pF. The reverse voltage V_r, established across the varactor, is equal to the difference between voltages V(t) and V_A induced at the sensing plate. The C-V curve shown in Figure 6 indicates that for low reverse voltage values the C-V relationship can be considered linear:

$$C_v = K \cdot V_r + C_{jO}, \tag{4}$$

where K is the line slope coefficient. For the reverse voltage range of 1SV277 from 0 to 2 V, the value of K = -1.8. Substituting formula 4 to

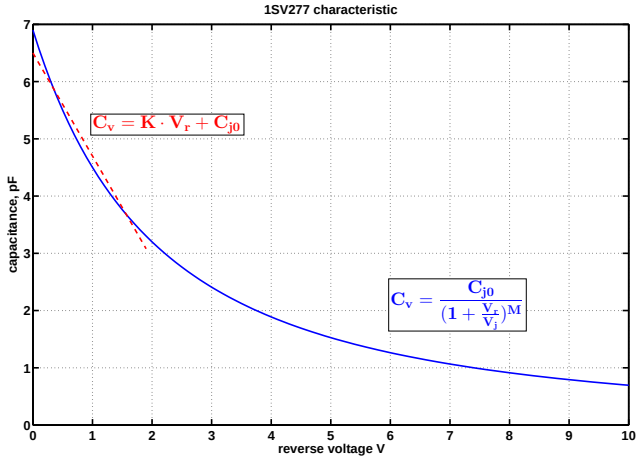

Fig. 6. Capacitance - voltage characteristic of 1SV277 varactor.

the equation for current 2 yields

$$I(s) = \frac{\frac{V \cdot \omega}{s^2+\omega^2} - \frac{V_o}{s}}{\frac{C_{j0}}{s} + \frac{K \cdot V \cdot \omega}{s^2+\omega^2} + R + \frac{1}{s \cdot C_{bp}}}, \tag{5}$$

Instead of solving this equation for the current I(s) (note again that the voltage V_o is treated as a DC voltage, as it is much "slower" than the carrier signal), it is much easier to simulate the variable capacitance element using the Analog Behavioral Modeling (ABM) module in PSpice [25], and demonstrate that the output of the linearized model is identical with the dual varactor model in Figure 3. The ABM functions allow for mathematical models implementation, and for the variable capacitance we use ABM2/I element out of the ABM PSpice library. Figure 7 shows implementation of the linear, voltage-dependent capacitor. The ABM function act as a current source I injecting the time-varying current proportional to changes of the voltage and capacitance, as outlined in [25]. The equation

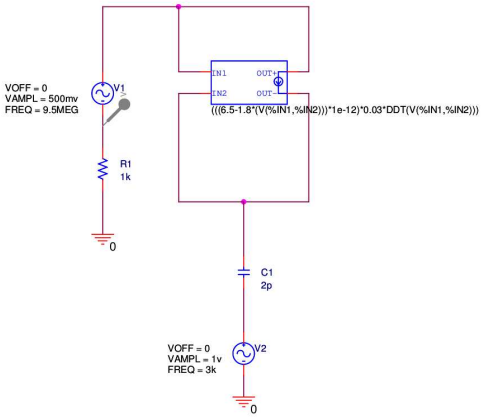

Fig. 7. PSpice equivalent circuit used in demonstrating variable capacitance concept.

linking voltage, capacitance and current is implemented as follows:

$$(((6.5-1.8\cdot(V(\%N1,\%N2)))\cdot 1e-12)\cdot 0.03\cdot DDT(V(\%N1,\%N2))) \tag{6}$$

which is identical to

$$I = C_v(V_r)\cdot\frac{dV_r}{dt} \tag{7}$$

The resulting current (Figure 8(a)) is identical with the current obtained with the varactor couple. It can be therefore concluded that the variable capacitance model theory is describing the action of the dual varactor front end sensing circuit. Moreover, it has been determined experimentally, and confirmed by using the PSpice model simulations, that by selecting steeper varactor C-V characteristic greater sensitivity can be obtained. Changing the slope coefficient K in the linearized model from -1.8 to -4 results in increased depth of AM modulation, which is shown in Figure 8(b).

The depth of modulation, or the modulation index, is proportional to the "gain" associated with the slope coefficient K. This allows for augmenting of the input voltage signal, induced on the sensor. One way of making the electric field sensors more sensitive is to utilize devices with C-V characteristics as steep as possible, bearing in mind that the modulation index should not exceed 100% to avoid distortion. Figure 9 presents an example of a pulse signal detected by the sensor's front end, before processing: The object used here was a plastic pellet dropped into a Faraday cup in front of the sensing plate - in this way the net charge of the pellet was determined.

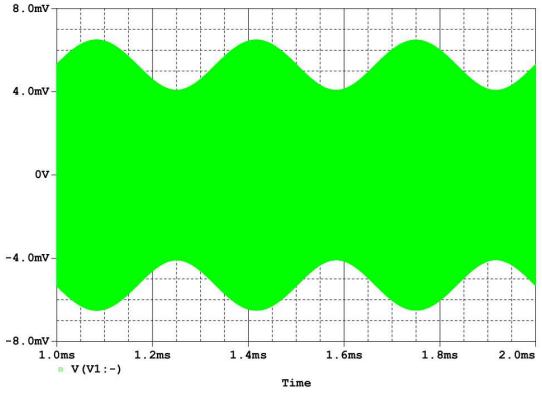

(a) K=-1.8.

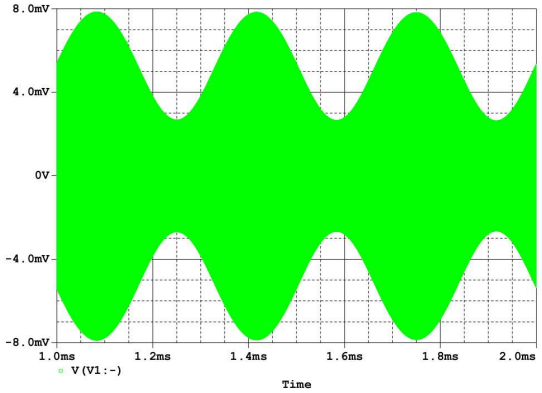

(b) K=-4.

Fig. 8. Simulated output voltage using linear model of the variable capacitance, 3 kHz, 1 V p-p input signal in place of the object under test signal.

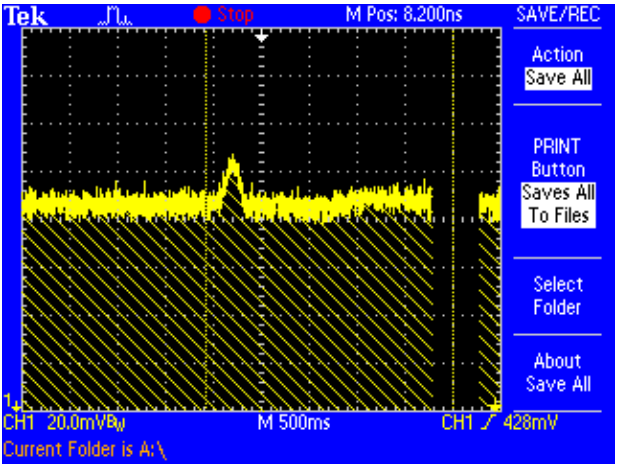

Fig. 9. Example oscillogram of the sensor's unprocessed signal. Sensor to object distance 0.09 m, object's charge 50 pC, amplitude of the detected signal 12 mV

III. Conclusions

Operation of the varactor electric field sensor was analyzed and discussed. The basic concept of the sensor can be best explained as having two capacitances in series, one between the sensing plate and the object under test, and the other capacitance is that of varactors. The varactor capacitance can be varied, making detection of DC electric fields possible. Moreover, due to nonlinear C-V characteristic the voltage induced on the sensing plate is converted to comparably larger current, thus increasing sensitivity.

IV. Acknowledgments

Parts of this work are supported by the Army Research Laboratory collaborative agreement W911NF-11-2-0067.

References

[1] H. Bassen and G. Smith, "Electric field probes–A review," *IEEE Trans. Ant. Propag.*, vol. 31, no. 5, pp. 710–718, 1983.

[2] M. Kanda, "Standard Probes for Electromagnetic Field Measurements," *IEEE Trans. Ant. Propag.*, vol. 41, no. 10, pp. 1349–1364, 1993.

[3] K. Munter, R. Pape, and J. Glimm, "Portable E-Field Strength Meter and its Traceable Calibration Up to 1 GHz Using a μ-TEM Cell," *IEEE Trans. Instrum. Meas.*, vol. 46, no. 1, pp. 549–550, 1997.

[4] D. M. Hull and S. J. Vinci, "Passive Aircraft Detection and Noncooperative Helicopter Identification Using Extremely Low Frequency (ELF) Electric Field Sensors," in *Enabling Technologies for Law Enforcement and Security*, A. T. DePersia and J. J. Pennella, Eds. International Society for Optics and Photonics, Dec. 1998, pp. 134–145.

[5] J. Cechak, "Detection of the Under-soil Intruder Activity," in *Proc. IX Conf. Unattended Ground, Sea, and Air Sensor Technologies and Applications*, vol. 6562, no. 656210. SPIE, 2007, p. 1=12.

[6] G. Cerri, F. Coacco, L. Fenucci, and V. Primiani, "Measurement of magnetic fields radiated from ESD using field sensors," *IEEE Transactions on Electromagnetic Compatibility*, vol. 43, no. 2, pp. 187–196, May 2001.

[7] J. Berthelier, M. Godefroy, F. Leblanc, M. Malingre, M. Menvielle, D. Lagoutte, J. Brochot, F. Colin, F. Elie, C. Legendre, P. Zamora, D. Benoist, Y. Chapuis, J. Artru, and R. Pfaff, "ICE, the electric field experiment on DEMETER," *Planetary and Space Science*, vol. 54, no. 5, pp. 456–471, Apr. 2006.

[8] Lord Kelvin, "Contact electricity of metals," *Philos. Mag.*, vol. 46, pp. 82–120, 1898.

[9] W. A. Zisman, "A New Method of Measuring Contact Potential Differences in Metals," *Rev. Sci. Instrum.*, vol. 3, no. 4, pp. 367–368, 1932.

[10] B. Lagel, I. D. Baikie, and U. Petermann, "A novel detection system for defects and chemical contamination in semiconductors based upon the Scanning {K}elvin Probe," *Surf. Sci.*, vol. 433 - 435, pp. 622–626, 1999.

[11] L. Kronik and Y. Shapira, "Surface photovoltage phenomena: theory, experiment, and applications," *Surf. Sci. Reports*, vol. 37, no. 1 - 5, pp. 1–206, 1999.

[12] P. Secker and J. Chubb, "Instrumentation for electrostatic measurements," *Journal of Electrostatics*, vol. 16, no. 1, pp. 1–19, Dec. 1984.

[13] S. Buchman, J. Mester, and T. J. Sumner, *Electrical Measurement, Signal Processing, and Displays, Chapter 8: Charge Measurement*, J. G. Webster, Ed. CRC Press, 2003.

[14] M. A. Noras, "Non-contact surface charge/voltage measurements. Fieldmeter and voltmeter methods," 2008. [Online]. Available: http://www.trekinc.com/pdf/3002-field-voltmeter.pdf

[15] A. Steinman and M. A. Noras, "Static Control Standards in the Semiconductor Industry," in *Proc. of EOS/ESD Symposium 2008*, p. 2008142.

[16] E. R. Jayaratne and T. S. Verma, "Environmental aerosols and their effect on the Earth?s local fair-weather electric field," *Meteorology and Atmospheric Physics*, vol. 86, no. 3-4, pp. 275–280, Jun. 2004.

[17] Simco Ion, "Ionizer measurements for critical static sensitive applications." [Online]. Available: http://technology-ionization.simco-ion.com/LinkClick.aspx?fileticket=Dj-g9tdjT3c%3d&tabid=546

[18] H. Herscovici, "Input Offset Voltage and Current in Varicap Diode Modulators," *IEEE Transactions on Instrumentation and Measurement*, vol. 28, no. 1, pp. 36–41, 1979.

[19] Hewlett Packard Ltd., *4140b pA meter/DC voltage source operation and service manual*, Hewlett-Packard, 1980.

[20] K. S. Cover, "Construction of a prototype {MOS} electrometer," *Rev. Sci. lnstrum.*, vol. 60, no. 8, pp. 2733–2739, 1989.

[21] M. A. Noras, "Electric Field Sensor Based on a Varactor Diode/MIS/MOS Structure," in *2010 IEEE Industry Applications Society Annual Meeting*. IEEE, Oct. 2010, pp. 1–3.

[22] M. A. Noras, S. P. Ramsey, and B. B. Rhoades, "Projectile detection using quasi-electrostatic field sensor array," *Journal of Electrostatics*, vol. 71, no. 3, pp. 220–223, Jun. 2013. [Online]. Available: http://www.mendeley.com/research/projectile-detection-using-quasielectrostatic-field-sensor-array/

[23] K. Mortenson, *Variable Capacitance Diodes*, 2nd ed. Artech House Inc., 1974.

[24] *1SV277 Datasheet*, Toshiba. [Online]. Available: http://www.semicon.toshiba.co.jp/info/

[25] *Application Note: A Nonlinear Capacitor Model for Use in the PSpice Environment*, Cadence, 2009. [Online]. Available: https://www.cadence.com/rl/Resources/application_notes/